PHYSICAL REVIEW D VOLUME 20, NUMBER 9 1 NOVEMBER 1979

Gluon jet production by the process $e^+e^- \to e^+e^- +$ gluon-gluon

Robert N. Cahn and John F. Gunion
Physics Department, University of California, Davis, California 95616
(Received 18 June 1979)

A novel means of producing a hadronic state evolving entirely from gluons is discussed. The gluons are generated by the collision of two virtual photons which couple to an intermediate quark loop. The rate for the process is calculated in the effective-photon approximation using the known QED cross section for photon-photon scattering. It is found that the two-gluon production process is about 8% as large as the basic two-photon process which creates a quark-antiquark pair. The cross sections are calculated as a function of the transverse momentum of the produced jet. At a center-of-mass energy squared for the incident electron and positron of $s = 900$ GeV^2, the two-gluon production rate is about 0.02 units of R (one unit of R is the point cross section for $e^+e^- \to \mu^+\mu^-$), if the jets are required to have at least 3 GeV/c of momentum transverse to the beam direction. At $s = 10000$ GeV^2, the corresponding rate is about 0.8 units of R.

INTRODUCTION

Quantum chromodynamics (QCD) is the theory of strong interactions in which the fundamental quanta are colored quarks and gluons. Since these particles are not observed directly, verification of QCD requires indirect tests. The study of e^+e^- annihilation into a single photon and subsequent conversion into a quark-antiquark pair provides a uniquely simple means of probing the pointlike quark structure and the hadronic materialization of a quark "jet." Analogous means for studying the gluons are more difficult to find. One possibility is the decay of a heavy $q\bar{q}$ resonance into two or three gluons.[1] This technique is, of course, limited by the availability of sufficiently heavy resonances.

Here we shall discuss a novel means for producing gluons and studying the hadronic development of a gluon jet: the "two-photon" process, $e^+e^- \to e^+e^-$ + gluon-gluon. In a "two-photon" process the incident electron and positron each emit a virtual photon and the two virtual photons collide to produce the final hadronic state. The simplest two-photon mechanism,[2] shown in Fig. 1(a), is $\gamma\gamma \to$ quark-antiquark. (For our purposes, the virtual photons may be regarded as real, to a very good approximation.)[3] The reaction $e^+e^- \to e^+e^-$ + gluon-gluon is mediated by quark loops, one diagram for which is shown in Fig. 1(b). In both cases, the final state consists of two hadronic jets. If gluon jets are, in practice, indistinguishable from quark jets, these processes cannot be disentangled; the gluon-gluon reaction will simply lead to an apparent increase in the cross section for the more frequent process of quark-antiquark production. A much more exciting possibility is that the gluon jets are quite different from quark jets[4] and can be separated from them on an event-by-event basis, at least in a reasonable fraction of the events. Then, since the gluons are well-defined dynamical objects, it should be possible to demonstrate that their appearance in two-photon events is the same as in heavy-resonance decays (should the latter be observed).

The existence of the process $e^+e^- \to e^+e^-$ + gluon-gluon is a direct test of QCD. The process arises at order α_s^2, where α_s is the strong coupling constant of QCD, and thus tests QCD at a detailed level much as the radiative processes of order α_s do, such as $e^+e^- \to q\bar{q}$ + gluon, discussed by Sterman and Weinberg and others.[5] If gluon jets are sufficiently distinctive, the existence and dynamics of the two-jet process discussed here may be easier to verify and provide a "cleaner" test of QCD than is possible for the above three-jet, single-photon annihilation-channel radiative process. Of course, it is crucial to note that exact predictions in QCD for short-distance processes of the types $e^+e^- \to e^+e^-$ + gluon-gluon and $e^+e^- \to e^+e^- + q\bar{q}$ can be given, just as it is possible for $e^+e^- \to q\bar{q}$ + gluon. The well-determined predictions for all these processes are to be contrasted with those for hadronic collisions where "bound-state" effects often obscure the simple pointlike, short-distance subprocesses. In the present case, the prediction of QCD is the same as that of the lowest-order pointlike calculation based on $\gamma\gamma \to$ gluon-gluon (via a quark loop) with the additional instruction to use the moving coupling constant $g_s(Q^2)$ at the gluon vertices. To avoid vector-dominance backgrounds, we will require that the gluons be produced at high transverse momentum, p_T, relative to the e^+e^- beam directions: "Q^2" is then $\sim 4p_T^2$, and vector-dominance backgrounds to $\gamma\gamma \to q\bar{q}$ and $\gamma\gamma \to$ gluon-gluon are suppressed[2] by about an order of magnitude for $p_T \gtrsim 3$ GeV/c.

The process $e^+e^- \to e^+e^-$ + gluon-gluon would be

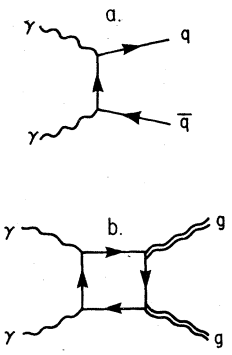

FIG. 1. (a) A diagram contributing to the process $\gamma\gamma \to q\bar{q}$. (b) A diagram contributing to the process $\gamma\gamma \to$ gluon-gluon. Other permutations of the attachments of the photons and gluons to the quark loop contribute also.

only a curiosity if the rate were so low that it could not be observed. In fact, as we show in detailed calculations below, this process will account for about 0.02 units of R [one unit of R is the cross section for $e^+e^- \to \mu^+\mu^- = 4\pi\alpha^2/(3s) = 87$ nb/s (in GeV^2)] at the PETRA/PEP energy, $s = 900$ GeV^2, which may be crudely converted into 4 events per day. At $s = 10\,000$ GeV^2, a reasonable value for the next generation of e^+e^- machines, the rate is about 0.8 units of R, or about 100 events per day. Here we have required that the produced gluon jet have at least 3 GeV/c of momentum transverse to the e^+e^- beam directions.

That the quark jets and gluon jets may be distinguished from each other has not been established experimentally. Theoretical studies[4] suggest that the gluon jets will have a significantly higher hadronic multiplicity for a given jet momentum. Since the process discussed here has a calculable cross section, it will be possible to test these speculations by searching for the appropriate number of higher-multiplicity events among the two-photon events observed.

A priori, the two-photon production of the gluon-gluon final state might be expected to be negligible. The cross section contains two more powers of the strong coupling constant α_s than does the cross section for the simpler process, $e^+e^- \to e^+e^- + q\bar{q}$, and it is reasonable to expect that the analytic expression would actually involve $(\alpha_s/\pi)^2$. However, it turns out that if we compare the leptonic analogs for the intermediate processes $\gamma\gamma \to \mu^+\mu^-$ and $\gamma\gamma \to \gamma\gamma$, the differential cross section at 90° for the $\gamma\gamma \to \gamma\gamma$ process is numerically about ten times larger than the above guess.[6] The color and charge factors enter differently for the $q\bar{q}$ and gg jet processes, resulting in a relative enhancement of the two-gluon final state by a factor of 2. However, since the q and $\bar{q}$ are distinguishable while the gluons are not, there is a compensating factor of 2. Altogether then, one estimates that the two-gluon final state is about 10% as common as the $q\bar{q}$ final state [the factor being approximately $10\times(\alpha_s/\pi)^2$]. More accurate calculations show that the ratio is nearer 8% for $\alpha_s = 0.3$.

In single-photon annihilation processes, the QED process $e^+e^- \to \mu^+\mu^-$ furnishes an appropriate reference cross section. For two-photon physics, a possible standard is $e^+e^- \to e^+e^- + \mu^+\mu^-$. Here, however, we must specify an additional variable. One possible choice is the invariant mass of the muon pair. The cross section for the two-photon process decreases very rapidly as a function of the muon-pair mass, at fixed incident e^+e^- energy. A more convenient variable is the transverse momentum of the muon relative to the incident beams (in the effective-photon approximation in which we work, the produced virtual photons have momentum along the beam direction, and thus the transverse momenta of the produced muons must just balance each other).

The importance of two-photon processes may be measured by asking, at a given value of s (the square of the e^+e^- energy): How many units of R appear in the reaction $e^+e^- \to e^+e^- + \mu^+\mu^-$ if the muons are required to have transverse momentum greater than a certain value p_T? This question can be answered rather simply and will provide a scale for the other reactions of interest. The result is simple because we can ignore the mass of the muon.

In Sec. II, we shall consider the process $e^+e^- \to e^+e^-$ + gluon-gluon in the limit in which the quarks in the closed loop, to which the gluons and virtual photons are attached, are treated as massless. At the same time, we shall examine the basic process $e^+e^- \to e^+e^- + q\bar{q}$ for massless quarks. Of course, this cross section is a simple multiple of the QED cross section $e^+e^- \to e^+e^- + \mu^+\mu^-$. The absence of quark masses will generate certain scaling relations between cross sections at different energies. Roughly speaking, cross sections expressed in dimensionless terms (units of R with $2p_T s^{-1/2}$ greater than a fixed amount) will scale except for a weak dependence on the initial energy $[\ln^2(s/4m_e^2)]$. This means it is quite easy to estimate the energy dependence of cross sections.

In Sec. III we shall reexamine the processes above, including quark masses and extending the list of quarks considered to include the b and hypothetical t quark. This is done by using the appropriate QED cross sections and inserting masses directly. The result is that the charmed quark enters with somewhat reduced strength, and the

b and t quarks contribute negligibly (and in some cases destructively). A discussion of the results and a review of some techniques which might be used to isolate the gluon events are given in Sec. IV.

II. MASSLESS-FERMION LIMIT

The two-photon process $e^+e^- \to e^+e^- + X$ is most easily treated in the equivalent-photon approximation, which relates the cross section for this process to the cross section for $\gamma\gamma \to X$. A convenient relation is[3]

$$d\sigma_{e^+e^- \to e^+e^- + X}(s) = \eta^2 \int_{\text{threshold}}^1 d\omega f(\omega) d\sigma_{\gamma\gamma \to X}(\omega s), \quad (1)$$

where

$$\eta = \frac{\alpha}{2\pi} \ln\left(\frac{s}{4m_e^2}\right) \quad (2)$$

(in the absence of triggering on the final e^+ and e^-) and

$$f(\omega) = [(2+\omega)^2 \ln(1/\omega) - 2(1-\omega)(3+\omega)]/\omega . \quad (3)$$

The function $f(\omega)$ represents an effective luminosity in the photon-photon channel for an invariant mass squared of the photon pair equal to a fraction ω of the overall e^+e^- center-of-mass energy squared. In this effective-photon approximation, the virtual photons are treated as if they were on-shell. Equation (1) applies not only to total cross sections, but to other appropriately defined cross sections as well. Specifically, it can be used so long as the cross section employed is invariant under boosts along the beam direction. A suitable differential cross section is

$$\frac{d\sigma}{dp_T}(s, p_T) = \frac{8\pi}{s^{1/2}} \left(\frac{s}{4p_T^2} - 1\right)^{-1/2} \frac{d\sigma}{d\Omega}(s, p_T) . \quad (4)$$

(A factor of 2 enters because, for fixed azimuthal angle, two values of θ contribute to the same p_T.) In Eq. (4) we have taken X to be a two-body system and p_T represents the transverse momentum of one of the two outgoing particles.

If there is no intrinsic mass scale for the process $\gamma\gamma \to X$ (as, for example, in $\gamma\gamma \to \mu^+\mu^-$, where the μ mass can be ignored at high energies except in the very forward direction), then, if we introduce the dimensionless variable

$$x_T = p_T/(\sqrt{s}/2) , \quad (5)$$

the differential cross section can be written in the form

$$\frac{d\sigma}{d\Omega}(s, p_T) = \frac{\alpha^2}{s} g(x_T^2) . \quad (6)$$

From Eqs. (1), (4), and (6), it follows that

$$\left(\frac{d\sigma}{dp_T}\right)_{(e^+e^- \to e^+e^- + X)}(s, p_T) = \frac{8\pi\alpha^2}{s^{3/2}} \eta^2 \int_{x_T^2}^1 d\omega\, \omega^{-3/2} f(\omega) \left(\frac{\omega}{x_T^2} - 1\right)^{-1/2} g\left(\frac{x_T^2}{\omega}\right) . \quad (7)$$

It is easier to compare the two-photon cross sections with the basic single-photon annihilation process if the result is expressed in units of R, that is, units of the cross section for $e^+e^- \to \mu^+\mu^-$: $\sigma_{\text{pt}} = 4\pi\alpha^2/3s$. In this way we obtain a dimensionless expression (now writing R for $\sigma/\sigma_{\text{pt}}$)

$$\frac{dR}{dx_T}(s, p_T) = \eta^2 3 \int_{x_T^2}^1 d\omega\, \omega^{-3/2} f(\omega) \left(\frac{\omega}{x_T^2} - 1\right)^{-1/2} g\left(\frac{x_T^2}{\omega}\right) . \quad (8)$$

As can be seen, this result is nearly independent of s for fixed x_T. The only s dependence comes from η, Eq. (2). The factor η^2 is 5.8×10^{-4} at $s = 900$ GeV^2, 7.1×10^{-4} at $s = 10\,000$ GeV^2, and 7.6×10^{-4} at $s = 20\,000$ GeV^2, when neither the outgoing e^+ nor e^- is triggered on.

Before calculating the two-gluon production, let us consider a simpler application of Eq. (8) which is of interest as a general measure of the importance of two-photon processes. For the purely leptonic process, the subprocess $\gamma\gamma \to \mu^+\mu^-$ has the differential cross section

$$\frac{d\sigma}{d\Omega}(s, p_T) = \frac{\alpha^2}{s} \left(\frac{s}{2p_T^2} - 1\right) . \quad (9)$$

We can then calculate the differential cross section

$$\frac{dR}{dx_T} = \eta^2 3 \int_{x_T^2}^1 d\omega\, \omega^{-3/2} f(\omega) \left(\frac{\omega}{x_T^2} - 1\right)^{-1/2} \left(\frac{2\omega}{x_T^2} - 1\right) \quad (10a)$$

$$\equiv \eta^2 h_{\mu\mu}(x_T) \quad (10b)$$

and, integrating this, we obtain

$$\int_{x_T}^1 \frac{dR}{dx_T'} dx_T' = \eta^2 \int_{x_T}^1 h_{\mu\mu}(x_T') dx_T' \quad (11a)$$

$$\equiv \eta^2 H_{\mu\mu}(x_T) . \quad (11b)$$

This latter expression determines the number of units of R for the process $e^+e^- \to e^+e^- + \mu^+\mu^-$ when the μ^+, say, is required to have $2p_T s^{-1/2}$ greater than x_T. The function $h_{\mu\mu}(x_T)$ and $H_{\mu\mu}(x_T)$ are shown in Figs. 3 and 4. (Approximate analytic expressions are given in the appendix.) For example, the cross section for producing a μ^+ with $p_T > 3$ GeV/c when $s = 900$ GeV^2 is $(5.8\times10^{-4})\times(2.7\times10^2) \approx 0.16$ units of R. If the same p_T is required, but

$s = 10\,000$ GeV^2, the result is $(7.1\times10^{-4})\times(1.25\times10^4)\approx 9$ units of R.

The simplest process for hadronic production in two-photon collisions is obtained by replacing the muons with quarks. If the quarks are treated as massless and if, as usual, point couplings are used, the cross section is simply related to that for muons, Eqs. (10) and (11). The only modification is multiplication by the sum of the fourth powers of the quark charges. If only u, d, and s quarks are included, the factor is $3\times(\frac{16}{81}+\frac{1}{81}+\frac{1}{81})=\frac{2}{3}$. If the c quark is included, the factor is $\frac{34}{27}$. For most kinematic regions of interest, the c quark contributes, but not as strongly as it would were it massless. Since unity is about halfway in-between $\frac{2}{3}$ and $\frac{34}{27}$, the muon-pair cross section is similar in magnitude to the $q\bar{q}$ cross section. A detailed discussion is given in the next section.

If the cross section for quark jets computed in this way is taken to include either a quark jet or an antiquark jet, there is an additional factor of 2 which must be included. If the cross section is taken to mean *events* rather than jets, this factor of 2 need not be included. We express our cross sections for *events*.

An analogous procedure can be used for the gluon-gluon production. The leptonic analog is $\gamma\gamma\to\gamma\gamma$, a process which is generated by a charged fermion loop. Light-by-light scattering has been carefully studied in quantum electrodynamics, although it has not been directly measured. Related diagrams do play an important role in g-2 calculations and in vacuum polarization in heavy muonic atoms. The full scattering amplitudes were calculated by Karplus and Neumann.[6] They were recalculated (and verified) by de Tollis,[7] who employed the Mandelstam representation. The forms given by de Tollis are easier to work with than those of Karplus and Neumann, and we have used de Tollis's expressions throughout our work.

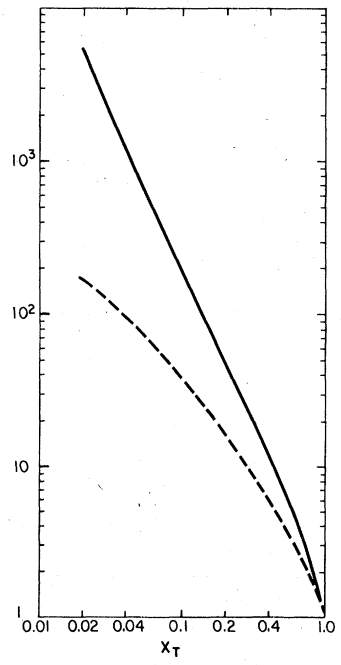

FIG. 2. The dimensionless functions which describe the differential cross sections for $\gamma\gamma\to\mu^+\mu^-$ and $\gamma\gamma\to\gamma\gamma$. The solid line gives the function $g(x_T)$ for $\gamma\gamma\to\mu^+\mu^-$. See Eqs. (5), (6), and (9). The dashed line gives the function $\tilde{g}(x_T)$ for $\gamma\gamma\to\gamma\gamma$. See Eq. (12).

For center-of-mass energies much higher than the mass of the fermion in the loop, and for scattering angles not too near the forward direction, the cross section for photon-photon scattering becomes independent of the fermion mass, and a form analogous to Eq. (6) may be written[7]:

$$\frac{d\sigma}{d\Omega}=\frac{\alpha^4}{s}\tilde{g}(x_T{}^2=\sin^2\theta)\,, \tag{12a}$$

$$\tilde{g}=\frac{1}{2\pi^2}[|1-2C_1(\sin^2\theta/2)|^2+|1-2C_1(\cos^2\theta/2)|^2 + |1-2C_2(\tan^2\theta/2)|^2+5]\,, \tag{12b}$$

$$C_1(x)=-\frac{1}{2}\left(\frac{1+x}{1-x}\right)(\ln x+i\pi) - \frac{1+x^2}{4(1-x)^2}[(\ln x)^2+2\pi i\ln x]\,, \tag{12c}$$

$$C_2(x)=\frac{1}{2}\left(\frac{x-1}{x+1}\right)\ln x-\frac{1}{4}\frac{1+x^2}{(1+x)^2}[\pi^2+(\ln x)^2]\,. \tag{12d}$$

Here θ is the center-of-mass scattering angle. The cross section given here is helicity averaged.

To compute the cross section for gluon-gluon production in the limit in which the quark masses are ignored, two powers of α are replaced by two powers of the strong coupling constant α_s. In addition, there is a color and charge factor associated with the various vertices. It is easy to see that this factor is

$$\tilde{F}=\left(\sum_{\text{flavors}=i}Q_i{}^2\right)^2\sum_{\substack{\text{gluon}\\ \text{types}=j,k}}\left(\mathrm{Tr}\frac{\lambda_j}{2}\frac{\lambda_k}{2}\right)^2 =(\tfrac{4}{9}N_{+2/3}+\tfrac{1}{9}N_{-1/3})^2 2\,. \tag{13}$$

The number of quark flavors with charge $\frac{2}{3}$ is $N_{+2/3}$ and the number of flavors with charge $-\frac{1}{3}$ is $N_{-1/3}$. Using the same notation, the factor which relates muon-pair production to $q\bar{q}$ production is

$$F=3(\tfrac{16}{81}N_{+2/3}+\tfrac{1}{81}N_{-1/3})\,. \tag{14}$$

If just u, d, and s are included, $F=\frac{2}{3}$ and $\tilde{F}=\frac{8}{9}$. If the c quark is included as well, $F=\frac{34}{27}$ and $\tilde{F}$

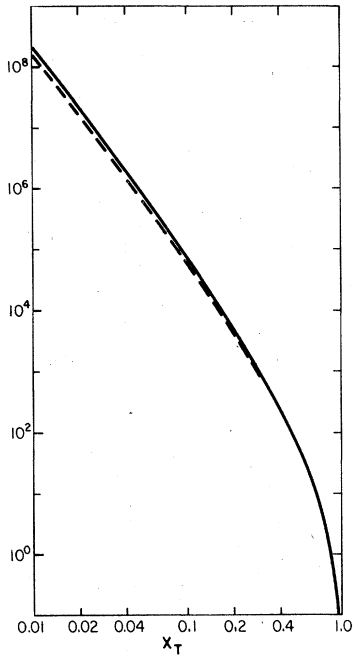

FIG. 3. The dimensionless functions which give the cross sections for jet production in the limit of massless fermions. The solid curve is $h_{\mu\mu}(x_T)$. See Eq. (10). The dashed curve is $h_{gg}(x_T)$. See Eq. (15).

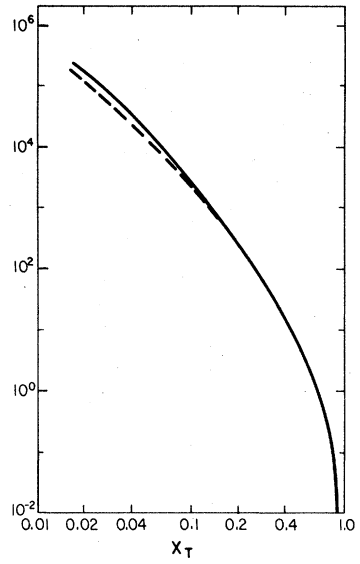

FIG. 4. The dimensionless functions which give the cross sections for the production of jets with x_T greater than a given amount. The solid curve is $H_{\mu\mu}(x_T)$. See Eq. (11). The dashed curve is $H_{gg}(x_T)$. See Eq. (16).

$= \frac{200}{81}$.

Using Eqs. (8) and (12) we can form expression analogous to those in Eqs. (10) and (11):

$$\frac{dR_{gg}}{dx_T} = \tfrac{1}{2}\alpha_s^2\eta^2\tilde{F}3\int_{x_T^2}^1 d\omega\,\omega^{-3/2}f(\omega) \times\left(\frac{\omega}{x_T^2}-1\right)^{-1/2}\tilde{g}\left(\frac{x_T^2}{\omega}\right) \tag{15a}$$

$$= \tfrac{1}{2}\alpha_s^2\eta^2\tilde{F}h_{gg}(x_T)\,, \tag{15b}$$

$$\int_{x_T}^1 \frac{dR_{gg}}{dx_T'}dx_T' = \tfrac{1}{2}\alpha_s^2\eta^2\tilde{F}\int_{x_T}^1 h_{gg}(x_T')dx_T' \tag{16a}$$

$$= \tfrac{1}{2}\alpha_s^2\eta^2\tilde{F}H_{gg}(x_T)\,. \tag{16b}$$

We have introduced a factor of $\frac{1}{2}$ into Eqs. (15) and (16) since we want the expression for R_{gg} to represent the number of events containing gluon jets of a certain transverse momentum, and each event contains two jets which would otherwise be counted separately. The functions $g(x_T)$, $\tilde{g}(x_T)$, $h_{gg}(x_T)$, and $H_{gg}(x_T)$ are shown in Figs. 2–4. It can be seen from the figures that the curves for $h_{\mu\mu}(x_T)$ and $h_{gg}(x_T)$ are quite similar, and consequently, so are the curves $H_{\mu\mu}(x_T)$ and $H_{gg}(x_T)$. This is simply a reflection of the near equality of $g(x_T)$ and $\tilde{g}(x_T)$ near $x_T = 1$. This region dominates the integrals in Eqs. (10a) and (15a) since it corresponds to the minimum value of ω where $f(\omega)$ is greatest. Thus, in the massless quark limit, the cross section for gluon-gluon production is the same as for muon-pair production with the same transverse momentum, except for an additional factor $\frac{1}{2}\alpha_s^2\tilde{F}$. The ratio of events for gluon-gluon production to $q\bar{q}$ production is $\frac{1}{2}\alpha_s^2\tilde{F}/F$ which is about $(\frac{1}{2})\times(0.3)^2 \times(\frac{4}{3}) = 0.06$ if only u, d, and s are included and $(\frac{1}{2})\times(0.3)^2\times(\frac{100}{51}) = 0.09$ if the c quark is included as well. We employ $\alpha_s(4p_T^2) = 0.3$ for $p_T \gtrsim 3$ GeV/c.

III. FINITE QUARK MASSES

We can incorporate the quark masses into our calculations in the following plausible manner. The underlying cross sections are calculated fixing the final state momenta, but inserting phenomenological quark masses into the exact expressions for the cross sections obtained from lowest-order perturbation theory. Essentially, the QED cross sections are used with phenomenological masses. While this is only an approximate treatment, it will clearly have the proper general features. The scaling relations which followed from Eq. (6) will no longer hold true since the cross sections can now depend on, say, the ratios of the quark masses squared to s. As a consequence, the s dependence of the cross sections will have to be displayed explicitly in this section.

For the simple $q\bar{q}$ production process, the final-state phase space is affected by the quark masses. For the gluon-gluon production, the quark masses

enter only through the loop calculation. It is intuitively clear that the introduction of a mass for the charmed quark will reduce the cross section for $c\bar{c}$ production. Since the gluon-gluon production receives coherent contributions from the various quarks, it is not predetermined what the effect will be, but it is not surprising that it also decreases the cross section. Similarly, the addition of b and t quarks must certainly increase total $q\bar{q}$ production. However, their introduction in some cases decreases the gluon-gluon production.

We have chosen the following quark masses for our calculations:

$$m_u = m_d = 0.3 \text{ GeV},$$
$$m_s = 0.5 \text{ GeV},$$
$$m_c = 1.5 \text{ GeV}, \tag{17}$$
$$m_b = 4.5 \text{ GeV},$$
$$m_t = 15 \text{ GeV}.$$

Our final results are not sensitive to small changes in these assignments. The massless limits of the differential cross sections, Eqs. (9) and (12), have been replaced with the full mass-dependent expressions.

The results of these calculations are shown in Figs. 5–8. Even at $s = 10\,000$ GeV^2, the b and t quarks contribute negligibly. The b quark is unimportant because of its small charge (which enters as the square or fourth power) and the t quark because of its large mass.

For $\gamma\gamma \to$ gluon-gluon we have employed a constant value $[\alpha_s(4p_T^2) = 0.3]$ for the coupling constant; α_s is in fact very slowly varying above "Q^2"$/\Lambda^2 = 4p_T^2/\Lambda^2 = 144$ (for $\Lambda = 0.5$ GeV). Using the differential results dR_{gg}/dp_T the reader can incorporate any desired variation of α_s. The scale Λ^2 is, as usual, not well determined, relative to the scale appropriate to deep-inelastic scattering QCD predictions, without a higher-order (α_s^3) calculation. We have not attempted this.

For the circumstances of this section we can define quantities analogous to those introduced in Eqs. (11b) and (16b):

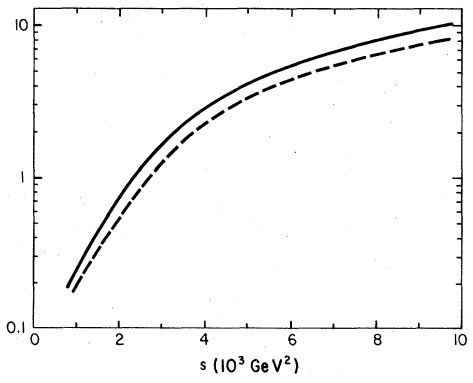

FIG. 5. The cross section, in units of R, for producing an event with a jet with transverse momentum greater than 3 GeV/c as a function of the e^+e^- center-of-mass energy squared s. The solid curve is for $q\bar{q}$ production. The dashed curve gives the cross section for gluon-gluon production multiplied by 10.

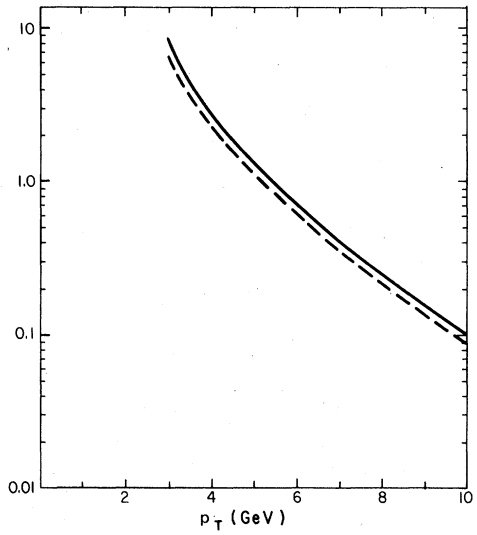

FIG. 6. The differential cross section dR/dp_T in (GeV/c)$^{-1}$ as a function of p_T in (GeV/c), for $s = 10^4$ GeV^2. The solid line gives the cross section for $q\bar{q}$ production. The dashed curve gives the cross section for gluon-gluon production multiplied by 10.

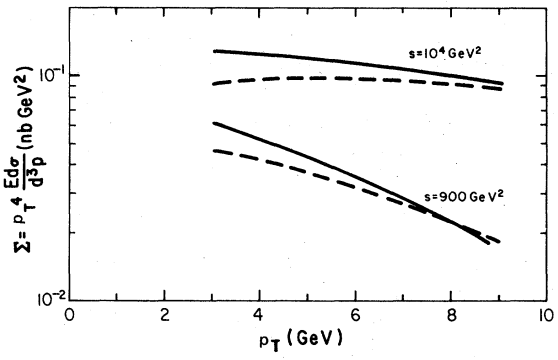

FIG. 7. The differential cross section Σ at $x_F = 0$, as a function of p_T for two values of s. Solid curves refer to $q\bar{q}$ production. Dashed curves refer to gluon-gluon production multiplied by 10.

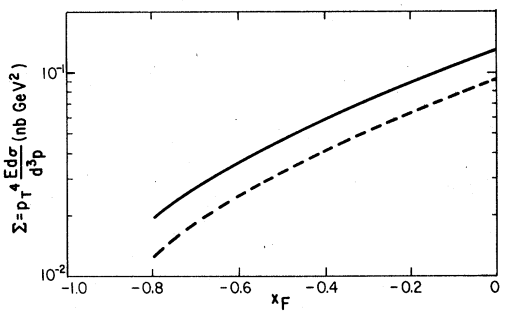

FIG. 8. The differential cross section Σ for $p_T = 3$ GeV/c at $s = 10\,000$ GeV^2, as a function of x_F. The solid curve refers to $q\bar{q}$ production. The dashed curve refers to gluon-gluon production multiplied by 10.

$$R_{q\bar{q}}(p_T = 3 \text{ GeV}, s) = \int_{p_T}^{\sqrt{s}/2} \frac{dR_{q\bar{q}}}{dp_T} dp_T , \tag{18a}$$

$$R_{gg}(p_T = 3 \text{ GeV}, s) = \int_{p_T}^{\sqrt{s}/2} \frac{dR_{gg}}{dp_T} dp_T . \tag{18b}$$

It is apparent from Fig. 5 that both $R_{q\bar{q}}$ and R_{gg} are rapidly increasing functions of s. From the arguments of the appendix, we expect them to increase faster than s for large s. In fact, between $s = 1000$ GeV^2 and $s = 10\,000$ GeV^2 the cross sections increase by about 40, so that at this latter energy, jets with more than 3-GeV transverse momentum are much more important than single-photon annihilation (unless there are many more quarks to be discovered). Even the gluon-gluon cross section is almost one unit of R, that is, as common as single-photon annihilation into muon pairs. With $\alpha_s = 0.3$, the integrated gluon-gluon cross section is about 8% as large as the two-photon $q\bar{q}$ production.

The addition of the c quark to the u, d, s quarks increases the $q\bar{q}$ production by a factor $\frac{17}{9} \cong 1.9$ in the massless limit. The more complete calculations of this section give an increase of about 1.7. Similarly, for the gluon-gluon production, the massless limit gives an increase of $\frac{25}{9} \cong 2.8$ while the actual calculations show an increase of about 2.4. As mentioned above, the b and t quarks contribute negligibly (and even negatively for gluon-gluon production).

The differential cross section dR/dp_T is shown in Fig. 6 for $s = 10^4$ GeV^2. As expected, the spectrum falls very rapidly with increasing p_T. The gluon-gluon cross section is approximately 8% of the quark-antiquark cross section.

Finally, we may examine the fully differential cross section $E(d\sigma/d^3p)$ as a function of p_T and x_F, where the latter is jet momentum parallel to the beam direction, divided by its maximum possible value, $\sqrt{s}/2$. This allows direct comparison[8] with the earlier results for quark-antiquark production of Ref. 2, where the quark masses were neglected. For convenience we actually plot $\Sigma = p_T^4 E(d\sigma/d^3p)$. In Fig. 7 we exhibit Σ as a function of p_T at $x_F = 0$ (90° c.m.) and in Fig. 8 we present Σ as a function of x_F at $p_T = 3$ GeV/c.

From the latter graph, we see that the ratio of gluon-gluon production to quark-antiquark production is a very slowly increasing function as $|x_F| \to 0$. The former graph illustrates the slow variation of Σ with p_T. By comparing the results at $s = 900$ GeV^2 with those given in Ref. 2, it is seen that only a modest decrease (15% maximum at the lowest p_T) has occurred as a result of including masses for the u, d, s, and c quarks.

IV. DISTINGUISHING GLUON AND QUARK JETS

From the preceding figures, it is apparent that the $q\bar{q}$ and gluon-gluon production processes have similar kinematic dependences. They will certainly not be distinguishable on this basis. One must hope that a gluon jet really has a very different structure from a quark jet. Numerous theoretical arguments support the view that once the jet momentum is substantial, the following characteristics of gluon jets should become apparent:

(a) The multiplicity should be $\frac{9}{4}$ ($= N_C/C_F$, a color group factor) times the multiplicity of a quark jet of the same momentum, on the average.[9]

(b) The distribution of single hadrons in the gluon jet should be steeper by a single power in $(1 - z)$, where $z = p_{\text{hadron}}/p_{\text{jet}}$. This prediction derives from the quark-counting rules.[10]

(c) The distribution of hadrons in the jet as a function of their transverse momentum relative to the jet axis should be broader for a gluon jet than for a quark jet[11]; typically, quantum chromodynamics predicts a normalized distribution

$$\frac{dN}{dk_T} \sim \frac{I(\epsilon)}{\pi} \frac{\bar{\alpha}(k_T)}{k_T} \left(\frac{\bar{\alpha}(Q/2)}{\bar{\alpha}(k_T)} \right)^{I(\epsilon)/\pi b} , \tag{19}$$

where I is a function of $\epsilon = \Delta\omega/Q$, the fraction of the quark or gluon jet energy emitted outside two oppositely directed cones of maximum transverse momentum $k_T^{\max} = Q\delta/2$, defined by half angle δ and jet momentum $Q/2$. The distribution applies for hadrons with $k_T < k_T^{\max}$. The function $I(\epsilon)$ depends on whether the jet is a quark or gluon jet:

$$I_{q\bar{q}} \propto C_F |\ln 2\epsilon| + O(1) , \tag{20a}$$

$$I_{gg} \propto N_C |\ln 2\epsilon| + O(1) , \tag{20b}$$

so that the ratio $I_{gg}/I_{q\bar{q}}$ is again controlled in first approximation by the group-theoretical factor $N_C/C_f = \frac{9}{4}$. The average value of k_T

$$\langle k_T{}^2\rangle = \int \frac{dN}{dk_T} k_T{}^2 dk_T \propto I(\epsilon)\bar{\alpha}(Q/2)\left[Q^2 + O\left(\frac{1}{\ln Q^2}\right)\right] \tag{21}$$

grows almost linearly with Q^2.

In summary, the gluon jets, on the average, should have higher multiplicity and should be shorter and broader than their quark jet counterparts with the same momentum.

Additional backgrounds will be generated by the processes discussed in Ref. 2. An example is $\gamma\gamma \to q\bar{q}$ + gluon. However, the most common configuration would have either the q or the $\bar{q}$ jet lying near the e^+e^- axis. A forward jet veto could be used to eliminate this and many other backgrounds with three or more jets.

Those events which are established as two-photon events and which have a two-jet structure[12] should be isolated and studied to determine whether they are in fact composed of two groups of events: one group with quark jets, such as those seen in single-photon annihilation events, and a second group about 8% as large with jets having a higher multiplicity and broader structure which would characterize the gluon jets.

ACKNOWLEDGMENT

We would like to acknowledge the support of the U. S. Department of Energy and the Alfred P. Sloan Foundation.

APPENDIX

We give here expressions for $h_{\mu\mu}(x_T)$ and $H_{\mu\mu}(x_T)$, Eqs. (10) and (11), accurate in the limit $x_T \to 0$. From Eq. (10),

$$h_{\mu\mu}(x_T) = \frac{3}{x_T{}^2}\int_1^{1/x_T{}^2} dz\, z^{-5/2}(z-1)^{-1/2}(2z-1)\left[\left(4\ln\frac{1}{z} + 4\ln\frac{1}{x_T{}^2} - 6\right) + x_T{}^2\left(4z\ln\frac{1}{z} + 4z\ln\frac{1}{x_T{}^2} + 4z\right)\right.$$
$$\left. + x_T{}^2\left(z^2\ln\frac{1}{z} + z^2\ln\frac{1}{x_T{}^2} + 2z^2\right)\right]. \tag{A1}$$

The term containing the next to the last large parentheses has an integrand which goes as $1/z$ for $z \to \infty$, so this term is smaller than the term in the first large parentheses by $\sim x_T{}^2$. A similar analysis applies to the third large parentheses. Thus we consider the approximation

$$h_{\mu\mu}(x_T) \simeq \frac{3}{x_T{}^2}\int_1^{\infty} dz\, z^{-5/2}(z-1)^{-1/2}(2z-1) \times\left(4\ln\frac{1}{z} + 4\ln\frac{1}{x_T{}^2} - 6\right). \tag{A2}$$

Now using

$$\int_0^{\infty} du\,(u+1)^{-5/2}(2u^{1/2} + u^{-1/2}) = \tfrac{8}{3}, \tag{A3}$$

we have

$$h_{\mu\mu}(x_T) \simeq \frac{3}{x_T{}^3}\frac{8}{3}\left(4\ln\frac{1}{x_T{}^2} - 6\right) - \frac{12}{x_T{}^3}\int_1^{\infty} dz\, z^{-5/2}(z-1)^{-1/2}(2z-1)\ln z. \tag{A4}$$

The final definite integral is

$$I = \int_1^{\infty} dz\, z^{-3}(2z-1)\left(1 - \frac{1}{z}\right)^{-1/2}\ln z = \int_1^{\infty} dz\, z^{-3}\ln z\,(2z-1)\left(1 + \frac{1}{2}\frac{1}{z} + \frac{3}{8}\frac{1}{z^2} + \cdots\right). \tag{A5}$$

Since

$$\int_1^{\infty} dz\, z^{-m}\ln z = \frac{1}{(m-1)^2},$$

we have

$$I = (2 - \tfrac{1}{4}) + \tfrac{1}{2}(\tfrac{2}{4} - \tfrac{1}{9}) + \tfrac{3}{8}(\tfrac{2}{9} - \tfrac{1}{16}) + \cdots \cong 2.02. \tag{A6}$$

Altogether then

$$h_{\mu\mu}(x_T) \cong \frac{1}{x_T{}^3}\left(32\ln\frac{1}{x_T{}^2} - 72\right). \tag{A7}$$

This is an excellent approximation for $x_T \lesssim 0.2$. From Eq. (A7) we obtain the approximation

$$H_{\mu\mu}(x_T) \cong \frac{16}{x_T{}^2}\ln\frac{1}{x_T{}^2} - 52\left(\frac{1}{x_T{}^2} - 1\right). \tag{A8}$$

[1]K. Koller and T. F. Walsh, Phys. Lett. 72B, 277 (1977); 73B, 504(E) (1978); Nucl. Phys. B140, 449 (1978); S. J. Brodsky *et al.*, Phys. Lett. 73B, 203 (1978); H. Fritzsch and K.-H. Streng, *ibid.* 74B, 90 (1978).

[2]S. J. Brodsky, T. DeGrand, J. Gunion, and J. Weis, Phys. Rev. Lett. 41, 672 (1978); Phys. Rev. D 19, 1418 (1979); K. Kajantie, in Proceedings of the LEP Workshop, Les Houches, France, 1978 (unpublished); in Proceedings of the XVIII Schladming Conference on Nuclear Physics, 1979 (unpublished); K. Kajantie and R. Raitio, Helsinki University Report No. HU-TFT-79-13 (unpublished).

[3]See, for a detailed treatment, S. J. Brodsky, T. Kinoshita, and H. Terazawa, Phys. Rev. D 4, 1532 (1971).

[4]S. J. Brodsky and J. F. Gunion, Phys. Rev. Lett. 37, 402 (1976); G. L. Kane and Y. P. Yao, Nucl. Phys. B137, 313 (1978); M. B. Einhorn and B. G. Weeks, *ibid.* B146, 445 (1978); K. Shizuya and S.-H. H. Tye, Phys. Rev. Lett. 41, 787 (1978); 41, 1195(E) (1978); K. Konishi, A. Ukawa, and G. Veneziano, Phys. Lett. 78B, 243 (1978); 80B, 259 (1979); G. Curci, M. Greco, and Y. Srivastava, CERN Report No. TH-2632, 1979 (unpublished).

[5]G. Sterman and S. Weinberg, Phys. Rev. Lett. 39, 1436 (1977); C. L. Basham *et al.*, *ibid.* 41, 1585 (1978); Phys. Rev. D 17, 2298 (1978); G. C. Fox and S. Wolfram, Phys. Rev. Lett. 41, 1581 (1978); Nucl. Phys. B149, 413 (1979); A. V. Smilga and M. I. Vysotskii, Nucl. Phys. B150, 173 (1979); R. K. Ellis and R. Petronzio, Phys. Lett. 80B, 249 (1979).

[6]The first complete calculation of $\gamma\gamma \to \gamma\gamma$ in QED was given in R. Karplus and M. Neumann, Phys. Rev. 80, 380 (1950); 83, 776 (1951).

[7]B. DeTollis, Nuovo Cimento 32, 757 (1964); 35, 1182 (1965).

[8]In Brodsky *et al.*, Ref. 2, the cross sections were calculated for *jets*, not events, so they were by a factor of 2 larger than the values calculated by our usual convention. For the cross sections Σ we adhere to the conventions of Brodsky *et al.*, Ref. 2, and include this additional factor of 2 in order to facilitate the comparison.

[9]S. J. Brodsky and J. F. Gunion, Ref. 4.

[10]R. Blankenbecler and S. J. Brodsky, Phys. Rev. D 10, 2973 (1974); J. F. Gunion, *ibid.* 10, 242 (1974).

[11]G. Curci, M. Greco, and Y. Srivastava, Ref. 4.

[12]We note that the background of the same topology, $\gamma\gamma \to M^*\bar{M}^*$, where two gluons are replaced by meson jets, has much stronger damping in p_T. It will be unimportant for $p_T > 3$ GeV/c. Fortunately, $\gamma\gamma \to gM^*$ is color forbidden.